Preparation of Functional Aptamer Films Using Layer-by-Layer Self-Assembly

ARTICLE *in* BIOMACROMOLECULES · MAY 2009

Impact Factor: 5.75 · DOI: 10.1021/bm8014126 · Source: PubMed

4 AUTHORS:

Yasir Sultan
Carleton University
12 PUBLICATIONS **152** CITATIONS
SEE PROFILE

Ryan P Walsh
Institut national de la recherche scientifique
27 PUBLICATIONS **520** CITATIONS
SEE PROFILE

Carlos Monreal
Agriculture and Agri-Food Canada
94 PUBLICATIONS **2,180** CITATIONS
SEE PROFILE

Maria C Derosa
Carleton University
63 PUBLICATIONS **2,041** CITATIONS
SEE PROFILE

Preparation of Functional Aptamer Films Using Layer-by-Layer Self-Assembly

Yasir Sultan,[†] Ryan Walsh,[†] Carlos Monreal,[‡] and Maria C. DeRosa*[,†]

Department of Chemistry, Carleton University, Ottawa-Carleton Chemistry Institute, 1125 Colonel By Drive, Ottawa, Ontario, Canada, K1S 5B6, and Eastern Cereal and Oil Seed Research Centre, Agriculture and AgriFood Canada, 960 Carling Avenue, Ottawa, Ontario, Canada, K1A 0C6

Received December 5, 2008; Revised Manuscript Received February 28, 2009

Advances in many aptamer-based applications will require a better understanding of how an aptamer's molecular recognition ability is affected by its incorporation into a suitable matrix. In this study, we investigated whether a model aptamer system, the sulforhodamine B aptamer, would retain its binding ability while embedded in a multilayer polyelectrolyte film. Thin films consisting of poly(diallyldimethylammonium chloride) as the polycation and both poly(sodium 4-styrene-sulfonate) and the aptamer as the polyanions were deposited by the layer-by-layer approach and were compared to films prepared using calf thymus DNA or a random single-stranded oligonucleotide. Data from UV−vis spectroscopy, quartz crystal microbalance studies, confocal microscopy, and time of flight secondary ion mass spectrometry confirm that the aptamer's recognition of its target is retained, with no loss of specificity and only a modest reduction of binding affinity, while it is incorporated within the thin film. These findings open up a raft of new opportunities for the development and application of aptamer-based functional thin films.

Introduction

The layer-by-layer (LbL) method[1] for the deposition of oppositely charged polyelectrolytes on solid substrates has been well-established as a convenient approach to the bottom-up assembly of multilayered polymer films.[2] The nature of the assembly process leads to precise, nanoscale control of film thickness and composition through the appropriate choice of the components, the number of layers, and the order of their deposition. Furthermore, LbL assembly is extremely versatile in terms of the choice of polyelectrolyte, allowing for these films to be tailored to their specific application. Biological macromolecules such as polypeptides/proteins,[3] polysaccharides,[4] nucleic acids,[5] and even viruses[6] can all serve as building blocks for these multilayer films. This allows for the preparation of biocompatible and biodegradable systems for a range of applications including those in sensing,[7] controlled release,[8] and biomedical technology.[9]

Aptamers are synthetic nucleic acids that fold into unique three-dimensional structures capable of binding tightly to a target of interest, with affinities and specificities that rival or even surpass those of monoclonal antibodies.[10] Unlike antibodies, which are temperature-sensitive and have a limited shelf life, aptamers are considerably more stable and can be transported at ambient temperatures. These nucleic acids can also be generated through an in vitro selection procedure[11] for a wide variety of targets, making them uniquely suited to effectively serve as receptors in sensor platforms.[12] Aptamers have been developed for a wide range of molecules, from drugs to proteins to very complex targets such as bacteria, tumor cell lines, and viruses.[13]

The potential for the use of aptamers as molecular recognition elements is clear, but to fully exploit these nucleic acids for the fabrication of biosensors and the development of other applications, aptamers will need to retain their functionality when embedded in or attached to a suitable matrix. Aptamers have been immobilized in a sol−gel,[14] tethered to cellulose,[15] and attached to a range surfaces[16] all without loss of their binding ability. Yet despite the great promise of LbL polyelectrolyte films for a wide range of applications, no work on the entrapment of aptamers within these films has been reported. The objective of this work was to determine whether the LbL approach could be used to prepare a robust aptamer film that maintained its affinity and specificity for the cognate target.

Here, we report on the first successful incorporation of a DNA aptamer into a multilayered polyelectrolyte thin film (Figure 1). We chose the sulforhodamine B (SB) aptamer[17] as our model system for this study. UV−vis spectroscopy, quartz crystal microbalance (QCM) studies, confocal microscopy, and time of flight secondary ion mass spectrometry (ToF-SIMS) all confirmed that the aptamer retained its recognition ability despite being embedded in the film. These films were simple to prepare and were stable and reusable. This opens up new possibilities for the development of aptamer-based functional films for use in biosensing, implant coatings, controlled-release, and many other applications.

Experimental Section

Materials. Quartz slides (75 × 25 mm) were purchased from VWR. Poly(diallyldimethylammonium chloride) (PDDA, M_w < 100000), poly(sodium 4-styrene-sulfonate) (PSS, M_w ~ 100000), calf thymus DNA (CT, sodium salt, type I), and sulforhodamine B (SB) were purchased from Sigma and were used as received. Tetramethylrosamine (TMR) was purchased from Invitrogen and was used as received. The sulforhodamine B aptamer (SA sequence: 5′-*CCG GCC TAG GGT GGG AGG GAG GGG GCC GG*-3′) and random oligonucleotide (RO sequence: 5′-*GAC CTA TGA TAG CAT CAG TCG CAT CAG TC*-3′) were synthesized on a merMADE 6 (Bioautomation Corporation) using standard phosphoramidite chemistry.

* To whom correspondence should be addressed. Phone: (613) 520-2600, ext. 3844. Fax: (613) 520-3749. E-mail: maria_derosa@carleton.ca.
[†] Carleton University.
[‡] Agriculture and AgriFood Canada.

10.1021/bm8014126 CCC: $40.75
Published on Web 04/22/2009

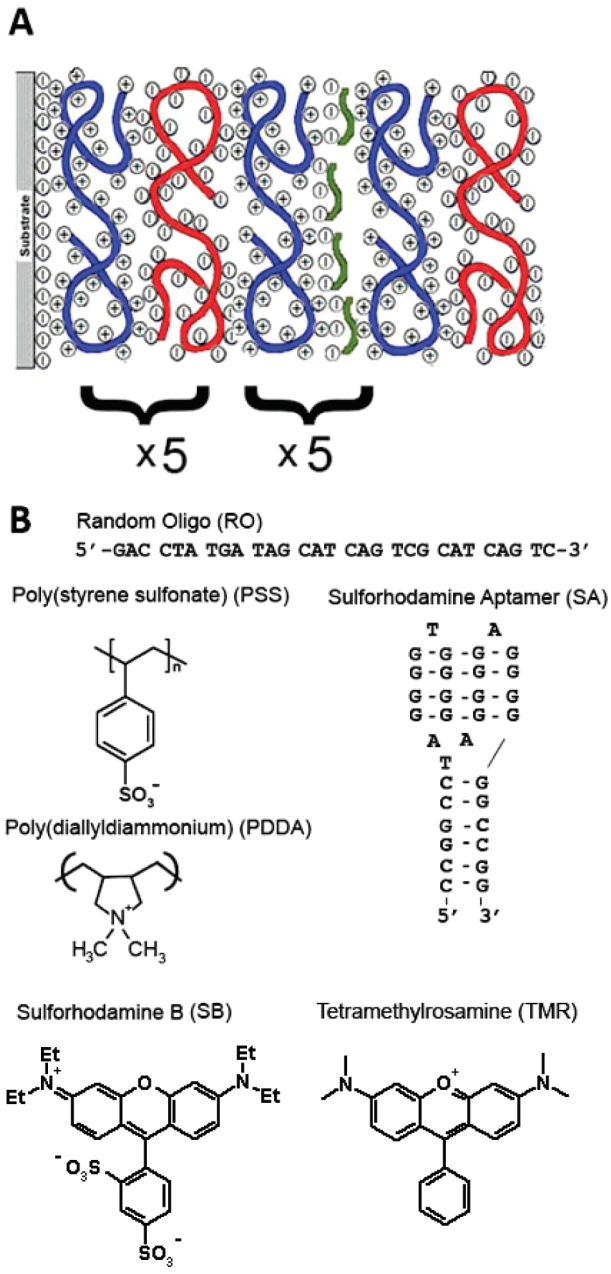

Figure 1. Experimental Overview. (A) Thin film composition. In PDDA/PSS/SA,[18] five bilayers of PDDA (blue) and PSS (red) are followed by five bilayers of PDDA and SA (green). The films are capped with a final bilayer of PDDA/PSS. The films PDDA/PSS/CT and PDDA/PSS/RO are prepared with a similar composition, except that calf thymus DNA (CT) or random oligonucleotide DNA (RO) is substituted for SA in the second five bilayers. PDDA/PSS films without any DNA were also prepared and used as controls. The film illustration was modified from ref 1. (B) Components of the experiment. The sequence of the random oligonucleotide (RO), the sequence and structure (showing the predicted g-quadruplex) of the sulforhodamine B aptamer (SA), and structures of the polyelectrolytes, PSS and PDDA, are presented. The structures of the target, sulforhodamine B (SB), and a related dye, tetramethylrosamine (TMR), are also shown.

Deposition of Polyelectrolyte Layers. Double deionized water was used for all experiments. Quartz slides were prepared by treatment with a solution of $H_2O_2/NH_3OH/H_2O$ (1:1:5) for 10 min at 70 °C. After pretreatment, the slides were washed with water and were then dipped successively in solutions of oppositely charged polyelectrolytes, starting with PDDA (5 mg/mL in 0.2 M NaCl) and then PSS (5 mg/mL in 0.2 M NaCl) for 20 min each. The slides were washed with copious amounts of water in between each deposition step. This procedure was repeated five times yielding five bilayers of PDDA and PSS (See Figure 1). Slides with only these bilayers (hereafter named[18] PDDA/PSS) served as controls in later experiments. For the films containing the sulforhodamine B aptamer (PDDA/PSS/SA), a random oligonucleotide (PDDA/PSS/RO), or calf thymus DNA (PDDA/PSS/CT), the next five bilayers were deposited with DNA as the anionic layer, in place of PSS. In each case, the slide was immersed in the DNA solution (6 μM for SA; 11 μM for RO; 0.04 μM for CT)[19] in 20 mM Tris-HCl (0.2 M NaCl, pH 7.4) for 20 min at room temperature. These films were terminated with an additional bilayer of PDDA/PSS to embed the DNA. Films were left to dry open to air at room temperature for at least 5 h before dye binding experiments were performed.

Dye Binding and Dissociation Constant (K_d) Experiments. Prior to dye binding, all films were heated in aqueous solution at 70 °C for 10 min to unfold any undesirable DNA conformations. Films were dipped in 2 mM sulforhodamine B (SB) or tetramethylrosamine (TMR) solution (0.1 M KCl) for 30 min and then washed with copious amounts of water until washings were no longer colored. UV/vis spectra of the films were obtained on a Cary 300 UV/vis spectrophotometer. To minimize electrostatic binding of the dye directly to the outermost layer of the polymer film, the film tested with negatively charged SB dye was terminated with PSS, while the film used for testing positively charged TMR was terminated with PDDA.

Reusability and stability of PDDA/PSS/SA was tested by immersing the slides in deionized water either at 40 or 70 °C for 10 min or 24 h at room temperature, and then examining the UV−vis spectrum for loss of the dye or DNA bands (570 and 260 nm, respectively). Films were then reimmersed in dye solution and binding was compared to the sample before heating by UV−vis.

Two types of dissociation constant experiments were performed. Initially, UV/vis spectroscopy was used as follows. PDDA/PSS/SA films were dipped in sulforhodamine B (0.1 M KCl) at concentrations of 0.001−10 mM for 30 min and washed with copious amounts of water before obtaining the UV/vis spectrum. The results were compared to those obtained using a quartz crystal microbalance (QCM) from Stanford Research Systems (QCM200, 5 MHz AT-cut quartz crystal oscillator with 0.1 s gate time). The quartz crystal was functionalized using the same preparation conditions as described for the quartz slides. Film growth was monitored by the change in relative frequency while carefully nulling any capacitance by manual control of the bias voltage required by the varactor. For the dissociation constant experiment, 1 mL solutions of varying SB concentrations (0.001−10 mM, 0.1 M KCl) were placed on the quartz crystal for 30 min, after which time the crystal was washed with copious amounts of water, dried under argon for 3 min, and the frequency change was noted. For both experiments, the dissociation constants were evaluated by minimizing the residuals values between calculated and observed experimental Δ absorbance or Δ frequency data using the solver feature of Microsoft Excel.[20]

Microscopy. All microscopy was performed in air. Confocal microscopy, to characterize the distribution of SB within the polymer films, was performed on a Zeiss LSM510 (532 nm, 3% laser intensity for the films PDDA/PSS/SA and PDDA/PSS/RO, 5% laser intensity for the PDDA/PSS/CT film) with a Plan-Acochromat 63x/1.4 Oil Dic objective with LP950 filter, exciting at 556 nm and collecting image data at 575 nm. Brightness (intensity) of the images was assessed by examining the images in Adobe Photoshop CS2 (V. 9.0.2), comparing the mean intensity values generated by the histogram tool, which graphs the number of pixels at each intensity level. Atomic force microscopy (AFM), to characterize surface topography of the films, was performed on a Veeco Instruments DI-3100 in both contact and tapping mode. AFM was also used to determine film thickness by creating a scratch on the polymer surface with a diamond etched knife on an Ntegra SFC050LNTF AFM head.

Time of Flight-Secondary Ion Mass Spectrometry (ToF-SIMS). A ToF-SIMS IV instrument from IonTOF GmbH was used to acquire compositional depth profiles of the films. Both positive and negative ion profiles were collected from several points on the surface. A Cs^+

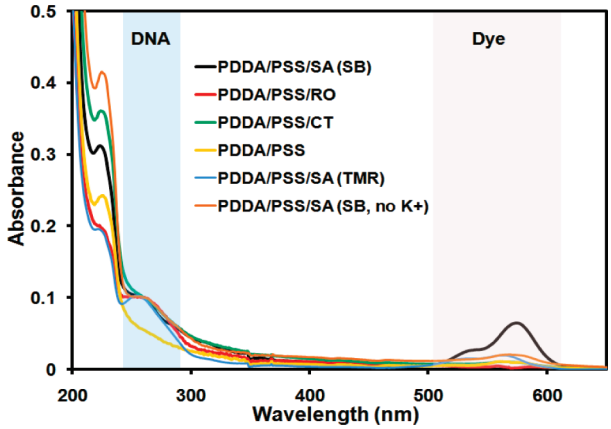

Figure 2. Overlay of UV−vis spectra of the polyelectrolyte films. DNA containing films are normalized at 260 nm. Black, PDDA/PSS/SA exposed to 2 mM sulforhodamine B (SB); red, PDDA/PSS/RO exposed to 2 mM SB; green, PDDA/PSS/CT exposed to 2 mM SB; yellow, PDDA/PSS alone exposed to 2 mM SB; blue, PDDA/PSS/SA exposed to 2 mM tetramethylrosamine (TMR); orange, PDDA/PSS/SA exposed to 2 mM SB, but without K^+. The regions of the spectra assigned to DNA and dye absorbances are highlighted. Upon immersion of the films in the dye solution, the aptamer films show the greatest degree of dye binding as evidenced by the largest peak at 570 nm.

Table 1. Comparisons of Dye, Polymer, and DNA Absorbance Values for the Films of this Study after Exposure to 2 mM Dye

sample composition	ratio[a] of SB dye peak height to polymer peak height (570:220 nm)	ratio[a] of SB dye peak height to DNA peak height (570:260 nm)
PDDA/PSS	0.12 (0.01)	
PDDA/PSS/CT	0.08 (0.01)	0.23 (0.02)
PDDA/PSS/RO	0.12 (0.03)	0.34 (0.09)
PDDA/PSS/SA (with K^+)	0.21 (0.06)	0.70 (0.01)
PDDA/PSS/SA (without K^+)	0.09 (0.01)	0.26 (0.03)

[a] Average of at least three measurements, standard deviation in parentheses.

ion beam at 500 eV primary energy was used for sputtering to collect negative secondary ions, and an O_2^+ ion beam with same energy was employed for the positive polarity. The sputter beams were rastered over an area of about 400 × 400 μm^2. The signal of the secondary ions was collected from the central area of about 200 × 200 μm^2 with 64 × 64 pixels. The analytical gun used to generate the secondary ions from the central area used a chopped 15 keV Ga ion beam in a high-current bunch mode. Charge compensation by electron flooding was also employed during profiling since the samples were nonconductive.

Results and Discussion

LbL self-assembly of polyelectrolyte films is emerging as a method of choice for the preparation of thin films for medicine, biology, and material science. As aptamers can be generated for nearly any target, incorporation of these nucleic acids as recognition elements within these multilayer films is of great interest. One concern, however, is that the electrostatic interaction of the aptamer with the surrounding polyelectrolyte matrix could potentially interfere with target recognition, especially in an aptamer that needs to be highly structured to effectively bind. For this reason, the sulforhodamine B aptamer, which adopts a g-quadruplex structure,[17] was chosen as our model for this study. To assess the binding ability of this aptamer when immobilized in a polymeric matrix, thin films were prepared using the LbL approach (Figure 1). Four types of films were prepared:[18] the

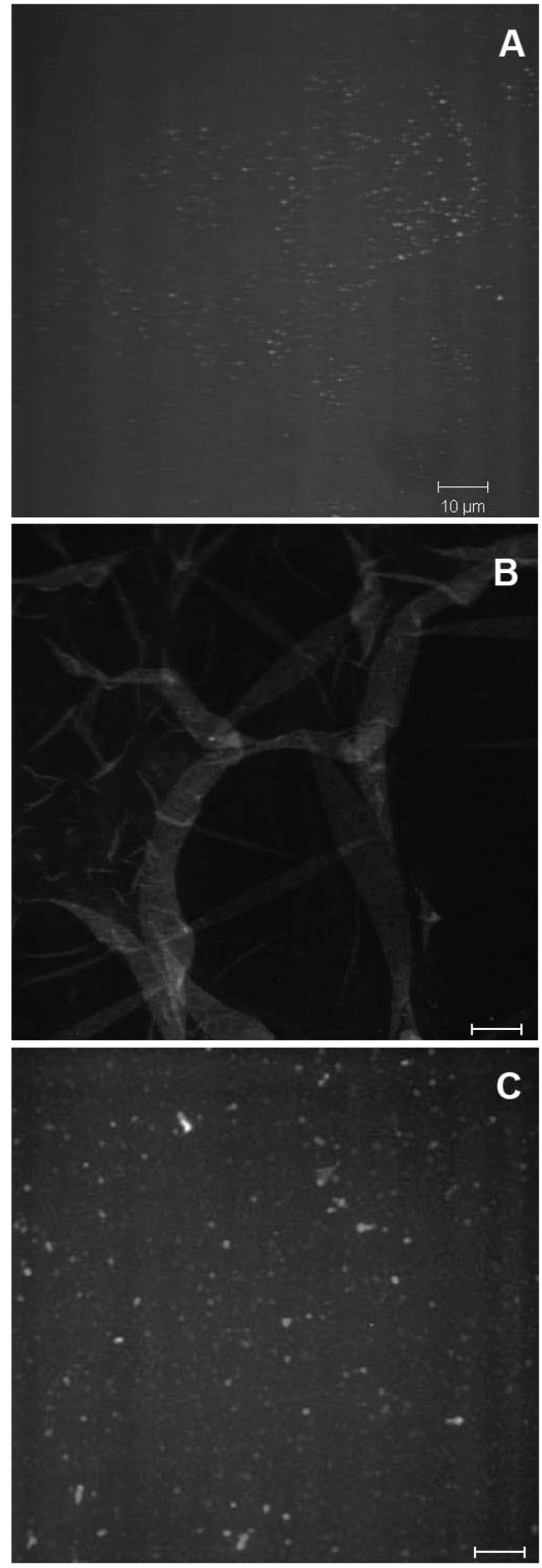

Figure 3. Confocal microscope images of the polyelectrolyte films after dye binding. Excitation 556 nm, emission 575 nm. White bars correspond to 10 μm (A) PDDA/PSS/RO, (B) PDDA/PSS/CT, and (C) PDDA/PSS/SA. The random oligonucleotide-containing film (PDDA/PSS/RO, A) shows few bright spots associated with the dye fluorescence. PDDA/PSS/CT films show very little dye fluorescence, with some localized nonspecifically within defects on the film surface. The film containing the aptamer (PDDA/PSS/SA, C) shows the brightest fluorescent areas associated with bound dye.

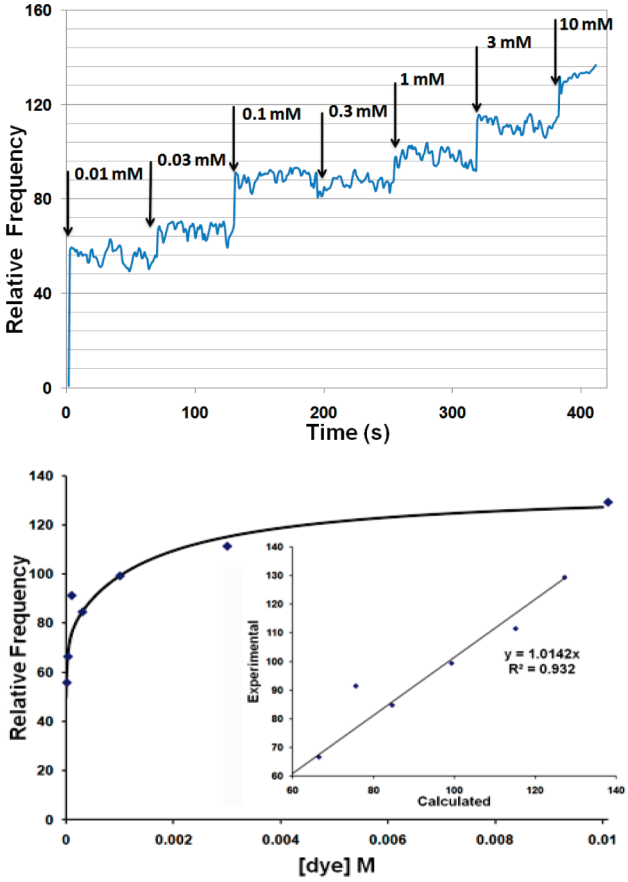

Figure 4. Representative data from QCM dissociation constant experiments. A PDDA/PSS/SA film on a quartz crystal was exposed to solutions of sulforhodamine B dye and the relative frequency was plotted vs the dye concentration. Top: Raw frequency data from the QCM experiment. Bottom: Plot of frequency over dye concentration. The line represents a two K_d model (see text). Inset: Values calculated using the two K_d model vs the experimental data.

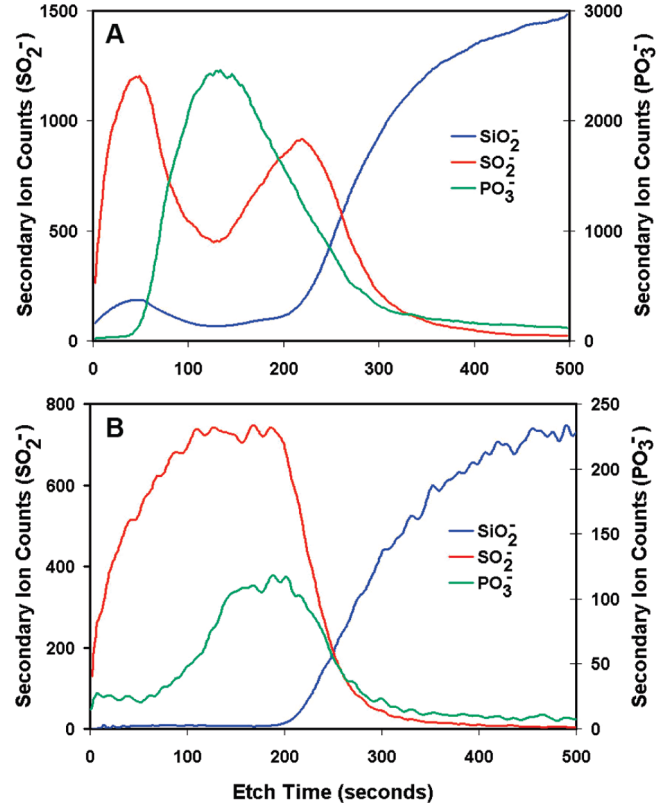

Figure 5. ToF-SIMS sputter depth profile of PDDA/PSS/SA before (A) and after (B) dye binding. Red, SO_2^-; green, PO_3^-; blue, SiO_2^-. The SO_2^- secondary ion is used to trace both PSS and SB, while the PO_3^- secondary ion is used to track the presence of the aptamer. The SiO_2^- ion counts have been reduced by a factor of 10 to fit on the same scale as the SO_2^-. (A) PDDA/PSS/SA alone: SO_2^- drops off dramatically as PO_3^- rises, and then rises again in the area directly above the slide surface. This trend was expected as the aptamer replaces PSS in the middle 5 bilayers of this film. (B) PDDA/PSS/SA and dye: SO_2^- counts reach a maximum at the same depth as do the DNA's PO_3^- counts, suggesting that the dye and the DNA are colocalized.

sulforhodamine B aptamer film, PDDA/PSS/SA, and three controls, PDDA/PSS (polymer layers only), PDDA/PSS/RO (containing a random oligonucleotide), and PDDA/PSS/CT (containing calf thymus DNA). In all films, five bilayers of PDDA and PSS were first deposited on a quartz slide. The growth of the film with each bilayer could be monitored via UV/vis (PSS ~ 220nm). For PDDA/PSS/SA, PDDA/PSS/RO, and PDDA/PSS/CT, the next five bilayers were deposited using DNA as the polyanionic electrolyte, either the sulforhodamine B aptamer, a nonspecific single-stranded random oligonucleotide, or calf thymus DNA, respectively. Growth of the films during DNA deposition could be monitored by UV−vis as well (260 nm). All films were terminated with an additional PDDA/PSS layer to embed the DNA within the film and also to minimize any electrostatic interaction between the charged dye and the film. Small molecules, such as the dye target, are known to diffuse through the layers of polyelectrolyte films, while larger biomolecules, nucleases for example, are not.[21] Thus, embedding the aptamer within the film should not impede dye access to the aptamer, but may serve to protect the aptamer from degradation. AFM was used to determine that the DNA-containing films were approximately 80 nm in thickness. This value is higher than what would be expected for a pure PDDA/PSS film at this salt concentration, demonstrating that the DNA layers have a sizable effect on film properties.[22]

UV−vis Spectroscopy. Given the strong absorbance of the SB dye in the visible region, UV−vis spectroscopy was employed as an initial measure of whether the target recognition of the aptamer was maintained while it was embedded within these polyelectrolyte films. Figure 2 is a comparison of the spectra for the various films after dye binding. Clearly, the spectrum of PDDA/PSS/SA shows a larger signal from the SB dye absorbance (~570 nm) than the controls. However, as the dye, DNA, and polymer peak intensities varied from film to film, ratios of dye peak height to polymer or DNA peak height were used to better quantify the affinity of the films for the target, as these ratios showed little variation from sample to sample (Table 1).

When PDDA/PSS films alone were tested for their ability to bind the dye nonspecifically, a small absorbance in the dye region was noted. This nonspecific binding could be attributed to the fact that the dye, being negatively charged, will likely have some affinity for the positively charged PDDA. In these films, the ratio of the dye peak intensity to polymer peak intensity was approximately 0.12. This serves as a baseline for nonspecific dye binding in these films. When either the random oligonucleotide or calf thymus DNA is included in these films, the amount of nonspecific binding (as measured by the dye to polymer ratio) is either less than or equal to the baseline value found in the polymer films alone. The aptamer-containing film, PDDA/PSS/SA, however, showed considerably stronger affinity for the dye, with a dye to polymer ratio of approximately 0.21.

Similarly, if the dye absorbance was compared to the DNA absorbance at 260 nm, the ratio of the peaks in the aptamer films was more than double that of the other films. Studies on the SA aptamer have indicated that the sequence forms a stacked g-quadruplex structure in the presence of K^+, but not Na^+, and that this structure is essential for maximum dye binding.[17] Indeed, heating the PDDA/PSS/SA films to unfold any undesirable DNA structures before immersion of the film in the dye solution with a high concentration of K^+ was required for efficient dye binding; films immersed in K^+-free dye solutions showed levels of dye binding that were comparable to controls. (see Figure 2 and Table 1) These data suggest that the aptamer in PDDA/PSS/SA retains its ability to form the g-quadruplex structure to recognize and bind the sulforhodamine B target, over and above the small nonspecific electrostatic interaction that the other films exhibit.

The effect of immobilization in the polyelectrolyte film on aptamer specificity was also investigated. In the original work on the SB aptamer, TMR dye was shown to be an inefficient competitor for binding, despite the structural similarities between the two molecules (see Figure 1).[17] When PDDA/PSS/SA films were exposed to TMR in 0.1 M KCl, only a low level of binding (dye to polymer ratio of 0.05, dye to DNA ratio of 0.17), similar to the amount in the K^+-free case, was detected (Figure 2). The specificity of the sulforhodamine aptamer was therefore unaffected by the polyelectrolyte matrix.

Confocal Microscopy. Given the intense fluorescence of the SB target, confocal microscopy could also be employed to assess the binding ability of the polyelectrolyte films. Confocal microscopy images of the thin films are shown in Figure 3. Images of PDDA/PSS/SA showed considerably more bright areas consistent with bound dye than did PDDA/PSS/RO or PDDA/PSS/CT. Given that the size of the bright spots is on the μm length scale, these are most likely the result of groups of aptamers binding to SB. The PDDA/PSS/SA and PDDA/PSS/RO films were taken under identical settings (for the case of the PDDA/PSS/CT films, however, laser intensity had to be increased by 2% in order to obtain usable images). When the standard photo processing software was used, the mean brightness of the PDDA/PSS/SA image (30 arbitrary units) was found to be twice that of the PDDA/PSS/RO image (14 arbitrary units). The CT DNA films were very inhomogeneous but, nevertheless, show the lowest mean brightness (1 arbitrary unit) and the least bright areas, and those that are present appear to be localized in defects on the films.[23]

Dissociation Constant Experiments (K_d). Dissociation constant (K_d) is generally used as a measure of an aptamer's binding affinity or sensitivity. In solution, the sulforhodamine B aptamer has a K_d of about 0.7 μM.[17] Dissociation constant experiments on our polyelectrolyte films, using absorbance changes at 570 nm with increasing dye concentration, proved difficult; in the PDDA/PSS/SA films, apparent dissociation constant values ranged from as low as 0.8 μM to as high as 3 mM (data not shown). While the lower value is consistent with the K_d for the sulforhodamine aptamer in solution, the higher value may be more representative of the nonspecific dye interaction with the polymer films. Quartz crystal microbalance (QCM) experiments were used in an attempt to clarify this issue. QCM is a powerful, quantitative technique that detects molecular recognition events through frequency changes associated with minute mass increases on the crystal surface. QCM has been used to determine K_d values for antibody−antigen and aptamer−target interactions.[24] PDDA/PSS/SA films were deposited onto the crystal and frequency changes detected with increasing concentrations of SB dye were evaluated (see Figure 4). The data fit best to a model with two binding affinities, a specific K_d of 16 uM and a nonspecific K_d of 1.5 mM, consistent with the values obtained using UV−vis. This suggests that the specific affinity of the aptamer has been only somewhat perturbed ($\sim$20 $\times$ higher K_d) by its incorporation into the polymer film. Data from control QCM K_d experiments on the PDDA/PSS/CT films fit to a single binding affinity in the low mM range (see Supporting Information). These results confirm that there is a nonspecific interaction between the films and the dye target. The high K_d of this interaction, however, makes this nonspecific binding unlikely to affect the detection of targets at low concentrations. Our current work is focused on eliminating or reducing this nonspecific interaction using other polyelectrolyte systems.

Time of Flight Secondary Ion Mass Spectrometry (ToF-SIMS). To further confirm the specificity of the dye for the aptamer within the polyelectrolyte layers, the investigation of dye localization as a depth profile, rather than as a bulk measurement, was attempted. ToF-SIMS was used to confirm specificity and colocalization of the dye and the aptamer within the films. ToF-SIMS measurements were taken as a depth profile over several points on the film to examine whether the dye was colocalized with the aptamer layers, which would be consistent with specific aptamer-target binding (Figure 5). The SO_2^- secondary ion was monitored as it was present in both the PSS polymer and the SB dye, and PO_3^- was chosen to track the presence of DNA. SiO_2^- was also monitored to demarcate the film/glass interface. In the absence of dye (Figure 5A), all the SO_2^- secondary ions are originating from the PSS within the film. The counts of SO_2^- secondary ion drop where the counts of PO_3^- ion rise. This is expected as there is no PSS in the layers of the film containing the aptamer. If SB dye had no affinity for the aptamer layers and was evenly distributed throughout the film, then after dye-binding the SO_2^- depth profile would be expected to show a similar trend. The regions of the film that contained both PSS and dye would show a higher SO_2^- ion count, and the regions of the film where PSS is replaced by SA would show a lower SO_2^- count originating from the dye alone. After dye-binding, however, the SO_2^- secondary ion trace does not follow that trend and instead now tracks with the PO_3^- ion (See Figure 5B). This suggests that dye is predominantly colocalized within the aptamer layers of the film. As both the DNA and the dye are negatively charged, this colocalization is unlikely to be due to a simple electrostatic interaction, and these findings further corroborate that the aptamer maintained its ability to recognize the dye while embedded in the film.

Stability and Reusability of Aptamer Films. Although DNA diffusion through polyelectrolyte films is expected to be minimal, a molecular beacon approach has recently shown that these multilayer films are somewhat permeable to short sequences of DNA.[25] Thus, PDDA/PSS/SA films were tested for their stability to leaching as well as their ability to be regenerated and reused. Little evidence of aptamer leaching was noted by examination of the peak at 260 nm when the films were left in deionized water over 24 h at room temperature. PDDA/PSS/SA films containing the dye were also subjected to immersion in deionized water at 40 and 70 °C; UV−vis spectra determined that the dye, but not the aptamer, could be removed from the films under these conditions (<1% loss of the signal at 260 nm). Dye binding after regeneration was found to be comparable to binding in the original films (>95% of the dye signal). Drying and air exposure also seemed to have little effect on the films. Aptamer-containing films left dry and open to air at room

temperature for over 3 months still showed binding affinity when reimmersed in dye solution.

Conclusions

When the sulforhodamine B aptamer as a model system was used, this study confirmed that an aptamer embedded in a polyelectrolyte matrix was still successful at binding its cognate target, with preserved specificity and only slightly perturbed affinity. This suggests that the sulforhodamine aptamer was able to retain its required g-quadruplex conformation while entrapped in the film. The multilayer polyelectrolyte films prepared by LbL assembly were found to be stable to aptamer leaching and reusable. Studies using more sensitive aptamer systems and employing different polyelectrolytes to decrease nonspecific target binding interactions with the polymer film are ongoing. The robust nature of these films, coupled with the ease with which they are prepared, indicates that LbL assembly is a practical and effective approach for the development of functional aptamer films. Future work will examine the application of these films as receptor elements for biosensing and controlled release.

Acknowledgment. M.C.D. thanks the Natural Sciences and Engineering Council of Canada (NSERC), the Canadian Foundation for Innovation (CFI), the Ontario Research Fund (ORF), and Carleton University for financial support. M.C.D. and C.M. thank the Alberta Agricultural Research Institute (AARI) for funding. Y.S. and C.M. thank Dr. Morris Schnitzer (Agriculture and Agri-Food Canada) for passing on his commitment to science. The authors acknowledge Dimitre Karpusov at ACSES (University of Alberta) for the ToF SIMS measurements, Ann-Fook Yang and Denise Chabot at Agriculture Canada for the confocal experiments, and Siddhartha Nandi and He (Shirley) Chang for help with the thin film preparation.

Supporting Information Available. Representative plot from QCM dissociation constant experiments on PDDA/PSS/CT. This material is available free of charge via the Internet at http://pubs.acs.org.

References and Notes

(1) Decher, G. *Science* **1997**, *277*, 1232–1237.
(2) Hua, F.; Lyov, Y. M. In *The New Frontiers of Organic and Composite Nanotechnology*; Erokhin, V., Ram, M. K., Yavuz, O., Eds.; Elsevier Press: New York, 2008; pp 1−44.
(3) (a) Benkirane-Jessel, N.; Lavalle, P.; Hübsch, E.; Holl, V.; Senger, B.; Haïkel, Y.; Voegel, J.-C.; Ogier, J.; Schaaf, P. *Adv. Funct. Mater.* **2005**, *15*, 648–654. (b) Picart, C.; Elkaim, R.; Richert, L.; Audoin, F.; Arntz, Y.; Da Silva Cardoso, S.; Schaaf, P.; Voegel, J.-C.; Frisch, B. *Adv. Funct. Mater.* **2005**, *15*, 83–94. (c) Lvov, Y.; Ariga, K.; Ichinose, I.; Kunitake, T. *J. Am. Chem. Soc.* **1995**, *117*, 6117–6123. (d) Kong, W.; Zhang, X.; Gao, M. L.; Zhou, H.; Li, W.; Shen, J. C. *Macromol. Rapid Commun.* **1994**, *15*, 405–409.
(4) (a) Richert, L.; Lavalle, P.; Vautier, D.; Senger, B.; Stoltz, J. F.; Schaaf, P.; Voegel, J.-C.; Picart, C. *Biomacromolecules* **2002**, *3*, 1170–1178. (b) Richert, L.; Lavalle, P.; Payan, E.; Shu, X. Z.; Prestwich, G. D.; Stoltz, J. F.; Schaaf, P.; Voegel, J. C.; Picart, C. *Langmuir* **2004**, *20*, 448–458.
(5) (a) Johnston, A. P. R.; Mitomo, H.; Read, E. S.; Caruso, F. *Langmuir* **2006**, *22*, 3251–3258. (b) Jewell, C. M.; Lynn, D. M. *Adv. Drug. Delivery Rev.* **2008**, *60*, 979–999. (c) Montrel, M. M.; Sukhorukov, G. B.; Petrov, A. I.; Shabarchina, L. I.; Sukhorukov, B. I. *Sens. Actuators, B* **1997**, *42*, 225–231. (d) Meyer, F.; Ball, V.; Schaaf, P.; Voegel, J.-C.; Ogier, J. *Biochem. Biophys. Acta, Biomembr.* **2006**, *1758*, 419–422.
(6) (a) Dimitrova, M.; Arntz, Y.; Lavalle, P.; Meyer, F.; Wolf, M.; Schuster, C.; Haïkel, Y.; Voegel, J.-C.; Ogier, J. *Adv. Funct. Mater.* **2007**, *17*, 233–245. (b) Yoo, P. J.; Nam, K. T.; Qi, J.; Lee, S.-K.; Park, J.; Belcher, A. M.; Hammond, P. T. *Nat. Mater.* **2006**, *5*, 234–240.
(7) Zhao, W.; Xu, J.-J.; Chen, H.-Y. *Electroanalysis* **2006**, *18*, 1737–1748.
(8) Lynn, D. M. *Soft Matter* **2006**, *2*, 269–273.
(9) Tang, Z. Y.; Wang, Y.; Podsiadlo, P.; Kotov, N. A. *Adv. Mater.* **2006**, *18*, 3203–3224.
(10) Bunka, D. H. J.; Stockley, P. G. *Nat. Rev. Microbiol.* **2006**, *4*, 588–596.
(11) (a) Tuerk, C.; Gold, L. *Science* **1990**, *249*, 505–510. (b) Ellington, A. D.; Szostak, J. W. *Nature (London)* **1990**, *346*, 818–822.
(12) (a) Willner, I.; Zayats, M. *Angew. Chem., Int. Ed.* **2007**, *46*, 6408–6418. (b) Tombelli, S.; Minunni, M.; Mascini, M. *Biomol. Eng.* **2007**, *24*, 191–200.
(13) Shamah, S. M.; Healy, J. M.; Cload, S. T. *Acc. Chem. Res.* **2008**, *41*, 130–138.
(14) Rupcich, N.; Nutiu, R.; Li, Y.; Brennan, J. D. *Anal. Chem.* **2005**, *77*, 4300–4307.
(15) Su, S.; Nutiu, R.; Filipe, C. D.; Li, Y.; Pelton, R. *Langmuir* **2007**, *23*, 1300–1302.
(16) Balamurugan, S.; Obubuafo, A.; Soper, S. A.; Spivak, D. A. *Anal. Bioanal. Chem.* **2008**, *390*, 1009–1021.
(17) Wilson, C.; Szostak, J. W. *Chem. Biol.* **1998**, *5*, 609–617.
(18) Film names were chosen for simplicity. The traditional naming convention for LbL films would give names as follows: PDDA/PSS = $(PDDA/PSS)_5$; PDDA/PSS/SA = $(PDDA/PSS)_5(PDDA/SA)_5(PDDA/PSS)$; PDDA/PSS/RO = $(PDDA/PSS)_5(PDDA/RO)_5(PDDA/PSS)$; PDDA/PSS/CT = $(PDDA/PSS)_5(PDDA/CT)_5(PDDA/PSS)$.
(19) The difference in concentrations of the SA, RO, and CT DNA are not expected to lead to large differences in the amount of DNA deposited in the film due to charge compensation effects. See Riegler, H.; Essler, F. *Langmuir* **2002**, *18*, 6694–6698.
(20) (a) Fylstra, D. H.; Lasdon, L.; Watson, J.; Waren, A. *Interfaces* **1998**, *28*, 29–55. (b) Nenov, I. P.; Fylstra, D. H. *Reliab. Comput.* **2003**, *9*, 143–159.
(21) (a) Antipov, A. A.; Sukhorukov, G. B.; Donath, E.; Möhwald, H. *J. Phys. Chem. B* **2001**, *105*, 2281–2284. (b) Yamauchi, F.; Koyamatsu, Y.; Kato, K.; Iwata, H. *Biomaterials* **2006**, *27*, 3497–3504. (c) El Haitami, A. E.; Martel, D.; Ball, V.; Nguyen, H. C.; Gonthier, E.; Labbé, P.; Voegel, J.-C.; Schaaf, P.; Senger, B.; Boulmedais, F. *Langmuir* **2009**, *25*, 2282–2289.
(22) McAloney, R. A.; Sinyor, M.; Dudnik, V.; Goh, M. C. *Langmuir* **2001**, *17*, 6655–6663.
(23) Although the nature of the features in the PDDA/PSS/CT films is unclear, they may be a result of deformation of the upper polymer layers due to the morphology of the CT DNA in the lower layers. Another possibility is that the CT film, after deposition, is more highly swollen than the other films (perhaps due to the size or charge on the CT DNA) and experiences rapid shrinking during the drying process that leads to this roughness. See Podsiadlo, P.; Michel, M.; Lee, J.; Verploegen, E.; Kam, N. W. S.; Ball, V.; Lee, J.; Qi, Y.; Hart, A. J.; Hammond, P. T.; Kotov, N. A. *Nano Lett.* **2008**, *8*, 1762–1770.
(24) Cooper, M. A.; Singleton, V. T. *J. Mol. Recognit.* **2007**, *20*, 154–184.
(25) Johnston, A. P. R.; Caruso, F. *J. Am.Chem. Soc.* **2005**, *127*, 10014–10015.

BM8014126